

# Evidence for a Non-Fermi-Liquid Phase in Ge-Substituted $\text{YbRh}_2\text{Si}_2$

J. Custers<sup>1</sup>, P. Gegenwart<sup>2,§</sup>, C. Geibel<sup>2</sup>, F. Steglich<sup>2</sup>, P. Coleman<sup>3</sup>, and S. Paschen<sup>1</sup>

<sup>1</sup>*Institute of Solid State Physics, Vienna University of Technology, Wiedner Hauptstr. 8-10, 1040 Vienna, Austria*

<sup>2</sup>*Max Planck Institute for Chemical Physics of Solids, 01187 Dresden, Germany and*

<sup>3</sup>*Center for Materials Theory, Rutgers University, Piscataway, NJ 08855, USA*

The canonical view of heavy fermion quantum criticality assumes a single quantum critical point separating the paramagnet from the antiferromagnet. However, recent experiments on Yb-based heavy fermion compounds suggest the presence of non-Fermi liquid behavior over a finite zero-temperature region. Using detailed susceptibility and transport measurements we show that the classic quantum critical system, Ge-substituted  $\text{YbRh}_2\text{Si}_2$ , also displays such behavior. We advance arguments that this is not due to a disorder-smearred quantum critical point, but represents a new class of metallic phase.

PACS numbers: 71.27.+a, 71.10.Hf, 72.15.Eb, 72.15.Qm

Quantum criticality in heavy fermion (HF) compounds has been a topic of great interest for more than a decade [1]. In the vicinity of a quantum critical point (QCP), HF materials display qualitative departures from the standard Landau Fermi liquid (LFL) behavior of conventional metals over a wide temperature ( $T$ ) range. Our failure to understand these phenomena constitutes a major unsolved problem in physics.

A key element in the debate about quantum criticality is whether the quantum critical physics of HF materials can be understood using a space-time generalization of classical criticality, often called ‘‘Hertz-Millis’’ theory [2, 3], or whether a new framework, evoking the critical breakdown of Kondo screening at the quantum critical point [4–8] is required. Recently, however, a new issue has arisen. Experiments on Yb-based HF systems, including  $\text{Yb}(\text{Rh}_{0.94}\text{Ir}_{0.06})_2\text{Si}_2$  [9],  $\text{YbAgGe}$  [10], and  $\beta\text{-YbAlB}_4$  [11] have observed the presence of non-Fermi liquid (NFL) behavior over a finite zero- $T$  region of the magnetic field ( $B$ )- or pressure ( $p$ )-tuned phase diagram, rather than at a single QCP. These observations raise the possibility that our underlying scenario for HF quantum criticality may need to be changed.

In this letter we re-investigate the low- $T$  magnetotransport and magnetic susceptibility properties of  $\text{YbRh}_2(\text{Si}_{0.95}\text{Ge}_{0.05})_2$  [12] to examine the earlier assumption of a single QCP. Together with  $\text{CeCu}_{5.9}\text{Au}_{0.1}$  [13] this material has played a major role in establishing the central properties of HF quantum criticality.

The  $T$ - $B$  phase diagram of the mother compound  $\text{YbRh}_2\text{Si}_2$  represents, with a well defined fan of NFL behavior in a LFL background [12], a particularly clear example of a quantum critical point. When a nominal concentration of 5 at% Si is substituted by Ge [14], this QCP was observed to move, for  $B \perp c$ , from 0.06 T further down towards 0.025 T [12]. Thus, a material situated, at  $B = 0$ , extremely close to its QCP appeared to be found. As will be shown below the NFL behavior of  $\text{YbRh}_2(\text{Si}_{0.95}\text{Ge}_{0.05})_2$  no longer emerges from a single point but occupies a finite segment of the  $B$  axis at  $T = 0$ . In addition the Kondo breakdown scale  $T^*$  [15, 16] is now detached from the zero  $T$  magnetic phase transi-

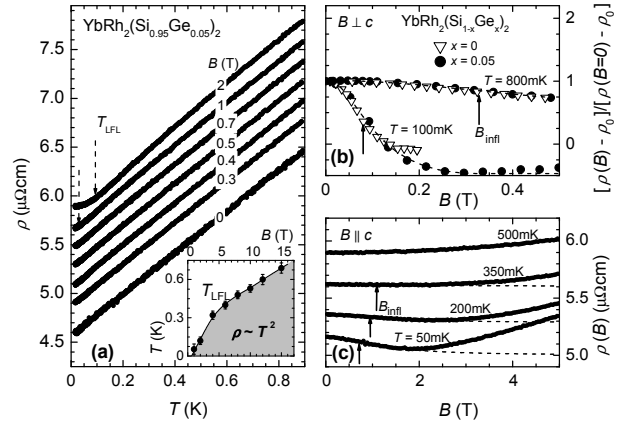


FIG. 1: Electrical resistivity of  $\text{YbRh}_2(\text{Si}_{0.95}\text{Ge}_{0.05})_2$ . (a) Low- $T$  resistivity for various  $B \parallel c$ . For clarity curves at  $B > 0$  are shifted by  $0.2 \mu\Omega\text{cm}$  with respect to each other. Below  $T_{\text{LFL}}$ , LFL behavior is recovered. Inset: Shaded area depicts region of LFL behavior determined from  $\rho(T)$ . The  $T_{\text{LFL}}$  line is a polynomial fit and serves as guide-to-the-eye. (b) Scaled isothermal magnetoresistance for  $B \perp c$  ( $\rho_0 = 4.51 \mu\Omega\text{cm}$ ). Data for pure  $\text{YbRh}_2\text{Si}_2$  (open symbols,  $\rho_0 = 1.81 \mu\Omega\text{cm}$ ) are shown for comparison. (c) Isothermal magnetoresistance for  $B \parallel c$ . The arrows denoted by  $B_{\text{infl}}$  mark the inflection points [16] of the fits to the data (full and dashed lines in (a) and (b), respectively) using the crossover function introduced in Ref. 15.

tion. This observation is of great interest in the context of new results for Co- and Ir-substituted  $\text{YbRh}_2\text{Si}_2$  [9] as well as on  $\text{CeIn}_3$  under high  $B$  [17], which also indicate a separation of  $T^*$  and  $T_N$  at zero  $T$ .

In Fig. 1(a) we show the  $T$  dependence of the electrical resistivity,  $\rho(T)$ , of  $\text{YbRh}_2(\text{Si}_{0.95}\text{Ge}_{0.05})_2$  for  $B \parallel c$  up to 2 T. A striking linearity of  $\Delta\rho(T)$  between at least 20 mK and 900 mK develops over the  $B$  range from zero to above 0.7 T. To our knowledge, such robust NFL behavior in a finite  $B$  range (factor of 45 in  $T$ , factor of 2.3 in  $B$  considering the expected crossover to a quadratic dependence at even lower  $T$  in the AFM state at  $B < B_{\text{c1}} = 0.3$  T, see Fig. 3) has not previously been observed in any HF compound [9–11]. In analogy with  $\text{YbRh}_2\text{Si}_2$  [16], the

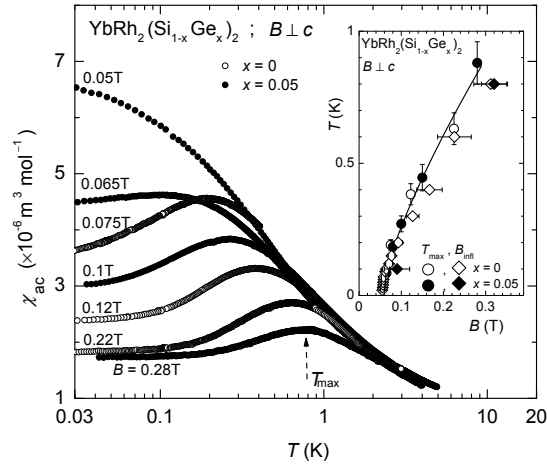


FIG. 2: Ac susceptibility of  $\text{YbRh}_2(\text{Si}_{1-x}\text{Ge}_x)_2$  for  $x = 0.05$  (full symbols) and, for comparison, for  $x = 0$  (open symbols). Inset: Positions of the maxima in iso- $B$   $\chi_{ac}(T)$  curves (circles) and of the inflection points [16]  $B_{\text{infl}}$  of  $\rho(B)$  isotherms (diamonds) of both samples. The power law  $(B - B_c)^{0.75}$  (solid line) with  $B_c = 0.06$  T is a good description of *all* data points.

resistivity  $\rho(B)$  isotherms have been examined. Clear crossover behavior is seen for  $B \perp c$  and  $B \parallel c$  which is characterized by inflection points [16] denoted as  $B_{\text{infl}}$  in Fig. 1(b) and Fig. 1(c), respectively. It is clear from these figures that  $B_{\text{infl}}$  increases with increasing  $T$ . Like Co- and Ir-substituted  $\text{YbRh}_2\text{Si}_2$  [9], the crossover behavior for the Ge-substituted compound investigated here is found to be almost identical with the one of pure  $\text{YbRh}_2\text{Si}_2$  (Fig. 1(b)).

This is further supported by another measure of the crossover scale  $T^*$ , the position  $T_{\text{max}}$  of maxima in iso- $B$   $\chi(T)$  curves [16], cf. Fig. 2. Like  $\rho(B)$ , also the  $\chi(T)$  data show that, while  $T_N$  is strongly suppressed upon substituting  $\text{YbRh}_2\text{Si}_2$  with Ge,  $T^*$  does not move (Fig. 2, inset).

Figure 3 summarizes all characteristic features of  $\text{YbRh}_2(\text{Si}_{0.95}\text{Ge}_{0.05})_2$  in a  $T$ - $B$  phase diagram. As indicated by the shaded area a finite range of NFL behavior at zero  $T$  appears between the critical fields  $B_{c1}$  and  $B_{c2}$  for the suppression of  $T_N$  and  $T^*$ .

In pure  $\text{YbRh}_2\text{Si}_2$ , the in- $T$  linear resistivity extends to the lowest accessible  $T$  (20 mK) at a single critical  $B$ , yet in  $\text{YbRh}_2(\text{Si}_{0.95}\text{Ge}_{0.05})_2$  this canonical behavior is violated, and instead, in- $T$  linear resistivity extends to the lowest  $T$  over a substantial  $B$  range. In isolation, this behavior might be dismissed as an anomaly. However, similar behavior has recently been observed also in other Yb-based HF compounds [9–11].

Conservatively, we might attribute these observations to disorder. In the Hertz-Millis theory, the in- $T$  linear resistivity of HF systems is itself attributed to disorder [18, 19]. Furthermore, disorder is expected to smear a well-defined QCP into a region [20].

However, various aspects speak against this conservative view point. Firstly, it is unlikely that the smearing

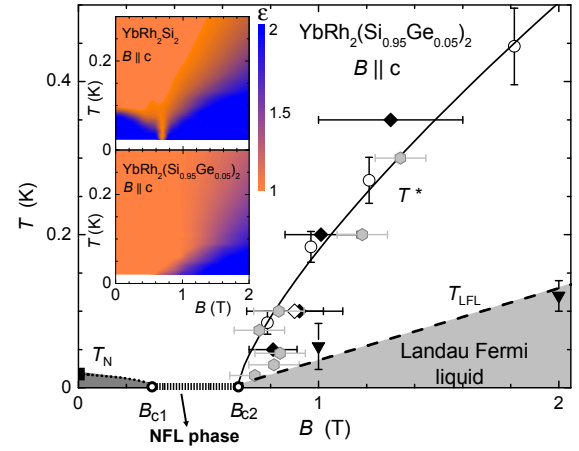


FIG. 3: (Color online) Phase diagram of  $\text{YbRh}_2(\text{Si}_{0.95}\text{Ge}_{0.05})_2$  for  $B \parallel c$ . Symbols represent  $B_{\text{infl}}$  ( $\blacklozenge$ ) and the upper boundary of LFL behavior ( $\blacktriangledown$ ). The dashed  $T_{\text{LFL}}$  line is the polynomial fit shown in the inset of Fig. 1(a). Data points from measurements with  $B \perp c$  are included by multiplying  $B$  with the factor 11:  $\diamond$  symbolizes  $B_{\text{infl}}$ ,  $\circ$  displays  $T_{\text{max}}$  from  $\chi_{ac}(T)$ . The solid  $T^*$  line is taken from the inset of Fig. 2. Hexagons represent  $T^*$  [16] (or  $T_{\text{Hall}}$  [15]) of  $\text{YbRh}_2\text{Si}_2$ .  $\blacksquare$  marks  $T_N$  observed by specific heat. The dotted  $T_N$  line indicates the typical evolution of  $T_N$  for  $\text{YbRh}_2\text{Si}_2$ ,  $T_N(B) = T_N(0)(1 - B/B_c)^{0.36}$  [9], using the respective parameters for  $\text{YbRh}_2(\text{Si}_{0.95}\text{Ge}_{0.05})_2$  ( $T_N(0) = 18$  mK,  $B_c = 11 \times B_c^{\perp c} \approx 0.3$  T) [12]. The hatched area  $0.3 \text{ T} \leq B \leq 0.66$  T marks the zero  $T$  NFL phase characterized by  $\Delta\rho \sim T$ . The inset compares the evolution of the resistivity exponent  $\epsilon$ , derived from the dependence  $(\rho - \rho_0) \sim T^\epsilon$  (see also Ref. 12), for  $\text{YbRh}_2\text{Si}_2$  (top) and  $\text{YbRh}_2(\text{Si}_{0.95}\text{Ge}_{0.05})_2$  (bottom) in the same  $B$  and  $T$  range.

of a QCP will be “asymmetric”. The position of the  $T^*$ -line in  $\text{YbRh}_2(\text{Si}_{1-x}\text{Ge}_x)_2$  and hence of the entrance into the LFL phase is not affected by going from  $x = 0$  to  $x = 0.05$  (see Refs. 15, 16 for the phase diagram of  $\text{YbRh}_2\text{Si}_2$ ); the NFL region in  $\text{YbRh}_2(\text{Si}_{0.95}\text{Ge}_{0.05})_2$  thus spreads only to the left of  $T^*$ . Secondly, the NFL power law dependencies are identical for  $\text{YbRh}_2(\text{Si}_{0.95}\text{Ge}_{0.05})_2$  and  $\text{YbRh}_2\text{Si}_2$  [12]. Thus, either both systems are disorder dominated or none. And finally, values for the normalized linear rise of resistivity  $\Delta\rho/\rho_0$  are, with  $\approx 4$  for  $\text{YbRh}_2(\text{Si}_{0.95}\text{Ge}_{0.05})_2$  [21],  $\approx 5$  for early  $\text{YbRh}_2\text{Si}_2$  samples [22], and  $\approx 20$  for the new generation of ultra-pure  $\text{YbRh}_2\text{Si}_2$  (where  $\rho = \rho_0 + AT^\alpha$  with  $\alpha = 1 \pm 0.2$  holds up to 20 K) [23], all beyond the maximum value of unity expected within the Hertz-Millis type scenario for disordered systems [18].  $\Delta\rho/\rho_0$  values more compatible with this scenario are observed for  $\text{CeCu}_{5.9}\text{Au}_{0.1}$  ( $\Delta\rho/\rho_0 \approx 0.5$ ) [24] and  $\text{YbAgGe}$  ( $\Delta\rho/\rho_0 \approx 1$ ) [10], values much larger than unity for  $\text{CeCoIn}_5$  ( $\Delta\rho/\rho_0 \approx 100$  for  $I \perp c$ ) [25]. Of course, the significance of  $\Delta\rho/\rho_0$  in estimating the role of disorder is questionable in systems as  $\text{YbRh}_2\text{Si}_2$  and  $\text{YbRh}_2(\text{Si}_{0.95}\text{Ge}_{0.05})_2$  where the Hertz-Millis theory fails [12, 15, 16].

A natural interpretation of our data, then, is that the  $B$ -region with in- $T$  linear resistivity corresponds to a well-defined metallic phase with unconventional

transport properties. The possibility of such “strange metal” phases that lie beyond a conventional LFL description has been discussed in a variety of theoretical contexts [8, 26–28]. One line of reasoning argues that the transition into the strange metal phase involves a partial Mott localization of the  $f$  quasiparticle degrees of freedom. Such a view is consistent with the  $T^*$  line that connects to the upper  $B$  edge of the strange metal phase. Anderson [27] has recently proposed the possibility of a “hidden Fermi liquid”, in which well-defined quasiparticles are present, but can not be created singly by the addition of external electrons.

The standard model of HF physics is based on Doniach’s “Kondo lattice hypothesis”, according to which deviations from the HF magnetic QCP are tuned by a single parameter  $K = T_K/J_H$ , the ratio of the single-ion Kondo temperature  $T_K$  to the nearest neighbor RKKY interaction  $J_H$ . As  $K$  is increased, a quantum phase transition QC1 takes place at some value  $K_c$  (see abscissa of Fig. 4,  $Q = 0$ ).

The apparent emergence of a strange metal phase in certain HF compounds leads us to propose a two parameter extension to the Doniach phase diagram which considers the interplay of the Kondo effect ( $K$ ) with the quantum zero point motion of the local moments ( $Q$ ). Related ideas have been previously considered by various authors [29–33]. To motivate this idea, we first consider a “drained Kondo lattice” ( $K = 0$ ), with only local moments coupled together on a lattice by a short-range antiferromagnetic (AFM) Heisenberg interaction. In isolation this lattice would develop an AFM ground state. However, by adding a frustrated second-neighbor coupling between the spins or, more abstractly, by reducing the size of the magnetic moment we can increase the strength of the quantum zero-point spin fluctuations. At some critical value  $Q_c$ , there is then a quantum phase transition QC2 where long-range magnetic order melts under the influence of zero-point spin fluctuations [34] to form a spin liquid (see ordinate of Fig. 4).

For the general case  $K \neq 0$ ,  $Q \neq 0$  we may link QC1 and QC2 via a single phase boundary (Fig. 4). However, this line is not the only feature in the phase diagram. When we turn on a small Kondo coupling between the conduction electrons and the spin liquid, the Kondo effect will not turn on instantly, since the spin liquid has a characteristic energy scale which will cut-off the Kondo logarithms. So, for small Kondo coupling, the spin liquid will co-exist with a small Fermi surface metal to form a “spin liquid metal”. The concept of a Kondo-stabilized spin liquid metal was first proposed in Ref. 35, but has more recently been discussed in connection with frustrated Kondo lattices [36], and as topologically distinct LFL phase of the Kondo lattice [6, 37]. Since the volume of the Fermi surface in the spin liquid metal is an invariant, the small and large Fermi surface states are topologically distinct phases, separated by at least one quantum phase transition. In the simplest scenario, a single quantum phase transition from a small to a large Fermi surface

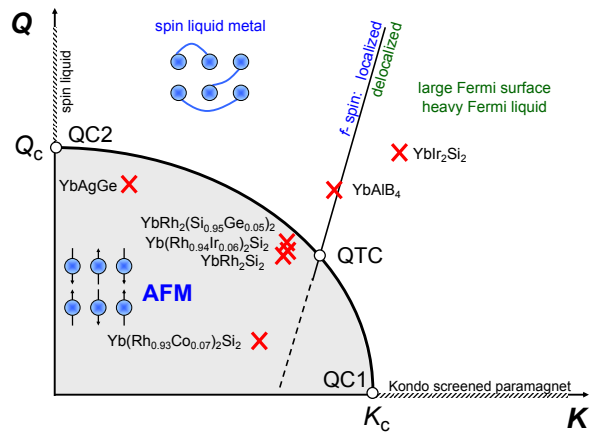


FIG. 4: (Color online) Generic phase diagram displaying the combined effects of Kondo coupling ( $K$ ) and magnetic frustration, or quantum zero point motion ( $Q$ ). For the location of compounds in the phase diagram (red crosses), see text.

must take place at some critical Kondo coupling  $K_c(Q)$ . In this way, the generalized magnetic-Kondo phase diagram must contain two *independent* quantum-critical lines - one where long range order develops, and another where the volume of the Fermi surface jumps. In general, these two lines will cross at a quantum tetra-critical point (QTC), where the  $f$  electrons localize at the same time as magnetic order develops. Tuning the parameters of the material in the vicinity of this QTC will, in this scenario, cause the two transitions to separate: for transitions that take place at  $Q$  values above the QTC, the AFM QCP will have the character of a localized magnetic QCP, whereas for  $Q$  values that lie below the QTC, the QCP will have the character of an itinerant (spin density wave) transition. Another interesting possibility which has been discussed is that, instead of a QTC, a line exists in the  $Q - K$  phase diagram on which the selective Mott transition and the AFM quantum critical point coincide [30].

In real HF materials, the precise relationship of  $p$  and  $B$  tuning the  $Q$  and  $K$  axes in our diagram will depend on microscopic details. For each material,  $p$  and  $B$  will define two generally non-orthogonal, but independent directions in the  $Q - K$  plane. Most of the existing data on Yb quantum critical systems have been interpreted assuming that  $B$  tuning can be identified with the  $K$  axis. The independent effect of doping or  $p$  must therefore at least have a finite component along the  $Q$  direction. With these assumptions, we can tentatively locate various Yb-based HF compounds in the  $Q - K$  plane.

According to its  $T - B$  phase diagram (Fig. 3)  $\text{YbRh}_2(\text{Si}_{0.95}\text{Ge}_{0.05})_2$  is situated in the AFM region, to the left of the localized-to-delocalized line. The low value of  $T_N$  (and the correspondingly low value of  $B_{c1}$ ) suggests that it is close to the AFM line.  $\text{YbRh}_2\text{Si}_2$  lies just to the left of the QTC in the phase diagram [15], while  $\text{Yb}(\text{Rh}_{0.94}\text{Ir}_{0.06})_2\text{Si}_2$  lies, due to its smaller  $T_N$ , at a higher values of  $Q$  [9], so that  $B$  tuning into the paramagnet

takes place via an intermediate spin liquid metal. By contrast, Co-substituted  $\text{YbRh}_2\text{Si}_2$  with a larger  $T_N$  lies at a lower value of  $Q$ , so that  $B$  tuning induces a delocalization of the  $f$  quasiparticles before the loss of magnetic order. The fact that  $B_{c2}$  is essentially the same for all these compounds is accounted for by positioning them around a line parallel to the localized-to-delocalized line. Their sequence along this line and their relative distances reflect the decrease of the chemical  $p$  (increase of the unit cell volume) towards the top [9, 12, 38].

The ground state of pure  $\text{YbIr}_2\text{Si}_2$  is a LFL. At the lowest  $T$  no signature of  $T^*$  was found in  $B$ -dependent Hall effect measurements [39]. In addition  $p$  experiments revealed that the paramagnetic ground state is stable up to  $p \approx 8$  GPa [40] leading us to place  $\text{YbIr}_2\text{Si}_2$  tentatively to the right of the  $f$ -spin localization line. We can also incorporate the parallel observations on  $\text{YbAgGe}$  and  $\text{YbAlB}_4$  into this framework.  $\text{YbAlB}_4$  is seen to enter a LFL phase almost immediately upon application of  $B$  [11], suggesting that this system lies just at the edge of the spin liquid metal phase.  $\text{YbAgGe}$  requires a substantial  $B$  for the destruction of the antiferromagnetism, but beyond the AFM QCP, it is seen to pass through a finite  $B$  range with linear resistivity (NFL region) [10]. High- $B$  effects like the putative Lifshitz transition in  $\text{YbRh}_2\text{Si}_2$  [41] at about 10 T fall outside the validity range of the phase diagram.

A central question raised by this discussion concerns the excitations of the proposed spin liquid metal. In particular, is the transport of charge, spin and/or heat carried by coherent fermions, or is a more radical description re-

quired? More detailed transport and spectroscopic measurements on Yb-based HF compounds with putative NFL phases [9–11] are clearly needed to help characterize the excitations in the  $B$  regime of linear resistance. It is equally important to experimentally quantify the theoretical parameters  $K$  and  $Q$ . This might be achieved with neutron scattering experiments in which the momentum independent quasielastic linewidth is a measure of the strength of the Kondo effect ( $K$ ) while the inelastic response at specific magnetic  $q$  vectors is a measure of the quantum zero point motion associated with antiferromagnetism ( $Q$ ) [42].

In conclusion, we have presented a set of transport and susceptibility measurements which strongly suggest the presence of a new metallic phase in magnetic field-tuned  $\text{YbRh}_2(\text{Si}_{0.95}\text{Ge}_{0.05})_2$ , nested between the antiferromagnetic and LFL ground states of this material. We have proposed a two-dimensional generalization of the Doniach phase diagram as a framework for interpreting this, and other recently observed cases of strange metal phases of similar character. Future experiments, based on pressure tuning could provide an important means of verifying these new ideas.

We gratefully acknowledge discussions with A. Nevidomskyy, S. Nakatsuji, and A. Millis. This work was supported by the ERC Advanced Grant n° 227378 (SP) and by NSF DMR 0907179 (PC).

<sup>§</sup>Present address: I. Physik. Institut, Georg-August-Universität Göttingen, 37077 Göttingen, Germany.

- 
- [1] H. v. Löhneysen et al., *Rev. Mod. Phys.* **79**, 1015 (2007).  
 [2] J. Hertz, *Phys. Rev. B* **14**, 1165 (1976).  
 [3] A. J. Millis, *Phys. Rev. B* **48**, 7183 (1993).  
 [4] P. Coleman et al., *J. Phys.: Condens. Matter* **13**, R723 (2001).  
 [5] Q. Si et al., *Nature* **413**, 804 (2001).  
 [6] T. Senthil, M. Vojta, and S. Sachdev, *Phys. Rev. B* **69**, 035111 (2004).  
 [7] T. Senthil et al., *Science* **303**, 1490 (2004).  
 [8] C. Pépin, *Phys. Rev. Lett.* **98**, 206401 (2007).  
 [9] S. Friedemann et al., *Nature Phys.* **5**, 465 (2009).  
 [10] S. L. Bud'ko, E. Morosan, and P. C. Canfield, *Phys. Rev. B* **69**, 014415 (2004).  
 [11] S. Nakatsuji et al., *Nature Phys.* **4**, 603 (2008).  
 [12] J. Custers et al., *Nature* **424**, 524 (2003).  
 [13] A. Schröder et al., *Nature* **407**, 351 (2000).  
 [14] The actual Ge-content of our single crystal is only about 2 at% (see caption of Fig. 1 in Ref. 12).  
 [15] S. Paschen et al., *Nature* **432**, 881 (2004).  
 [16] P. Gegenwart et al., *Science* **315**, 969 (2007).  
 [17] S. E. Sebastian et al., *PNAS* **106**, 7741 (2009).  
 [18] A. Rosch, *Phys. Rev. Lett.* **82**, 4280 (1999).  
 [19] T. Moriya and T. Takimoto, *J. Phys. Soc. Jpn.* **64**, 960 (1995).  
 [20] J. A. Hoyos and T. Vojta, *Phys. Rev. Lett.* **100**, 240601 (2008).  
 [21] O. Trovarelli et al., *Physica B* **312-313**, 401 (2002).  
 [22] O. Trovarelli et al., *Phys. Rev. Lett.* **85**, 626 (2000).  
 [23] T. Westerkamp, dissertation, TU Dresden, Germany, 2009.  
 [24] H. v. Löhneysen et al., *Phys. Rev. Lett.* **72**, 3262 (1994).  
 [25] X. Tang et al., *J. Mater. Res.* **16**, 837 (2001).  
 [26] T. Senthil, *Phys. Rev. B* **78**, 035103 (2008).  
 [27] P. W. Anderson, *Phys. Rev. B* **78**, 174505 (2008).  
 [28] A. H. Nevidomskyy and P. Coleman, *Phys. Rev. Lett.* **102**, 077202 (2009).  
 [29] S. Burdin, D. R. Grempel, and A. Georges, *Phys. Rev. B* **66**, 045111 (2002).  
 [30] Q. Si, *Physica B* **378-380**, 23 (2006).  
 [31] E. Lebanon and P. Coleman, *Phys. Rev. B* **76**, 085117 (2007).  
 [32] M. Vojta, *Phys. Rev. B* **78**, 144508 (2008).  
 [33] T. T. Ong and B. A. Jones, *Phys. Rev. Lett.* **103**, 066405 (2009).  
 [34] See, for example, P. Chandra and B. Douçot, *Phys. Rev. B* **38**, 9335 (1988).  
 [35] P. Coleman and N. Andrei, *J. Phys.: Condens. Matter* **1**, 4057 (1989).  
 [36] S. Nakatsuji et al., *Phys. Rev. Lett.* **96**, 087204 (2006).  
 [37] M. Vojta and S. Sachdev, *Phys. Rev. Lett.* **83**, 3916 (1999).  
 [38] M. E. Macovei et al., *J. Phys.: Condens. Matter* **20**, 505205 (2008).  
 [39] M. Kriegisch et al., *Physica B* **403**, 1295 (2008).  
 [40] H. Q. Yuan et al., *Phys. Rev. B* **74**, 212403 (2006).  
 [41] P. M. C. Rourke et al., *Phys. Rev. Lett.* **101**, 237205 (2008).  
 [42] W. Montfrooij et al., *Phys. Rev. Lett.* **91**, 087202 (2003).